Journal of Bioenergetics and Biomembranes, Vol. 30, No. 1, 1998

Time-Resolved Resonance Raman Investigation of Oxygen Reduction Mechanism of Bovine Cytochrome *c* Oxidase

Teizo Kitagawa[1] and Takashi Ogura[1]

Received August 19, 1997; accepted August 26, 1997

Six oxygen-associated resonance Raman bands were identified for intermediates in the reaction of bovine cytochrome *c* oxidase with O_2 at room temperature. The primary intermediate, corresponding to Compound A of cryogenic measurements, is an O_2 adduct of heme a_3 and its isotope frequency shifts for $^{16}O^{18}O$ have established that the binding is of an end-on type. This is followed by two oxoheme intermediates, and the final intermediate appearing around 3 ms is the Fe–OH heme. The reaction rate between the two oxoheme intermediates is significantly slower in D_2O than in H_2O, suggesting that the electron transfer is regulated by proton translocations at this step. It is noted that the reaction intermediates of oxidized enzyme with hydrogen peroxide yield the same three sets of oxygen isotope-sensitive bands as those of oxoheme intermediates seen for O_2 reduction and that the O–O bond has already been cleaved in the so-called peroxy form (or 607 nm form).

INTRODUCTION

Terminal oxidases of the mitochondrial respiratory chain commonly contain two copper complexes (Cu_A and Cu_B) and two heme-A groups (heme *a* and heme a_3) as redox centers.[1] The Cu_A center, which has a mixed valence Cu_2S_2 cluster in the oxidized state with a CT band around 830 nm, receives electrons from cytochrome *c* and gives them to heme *a*. Heme *a* (Fe_a) is of a six-coordinate low-spin type and works for electron transfers from Cu_A to heme a_3, while heme a_3 (Fe_{a3}) is of a five-coordinate high-spin type and provides the catalytic site for O_2 reduction. Cu_B lies at 4.5 Å apart from Fe_{a3} and is antiferromagnetically coupled with it in the resting state, being EPR silent, while the role of Cu_B remains to be clarified. Full reduction of O_2 to H_2O requires four electrons and four protons. This reaction, catalyzed by the heme a_3, proceeds in a stepwise fashion in a respiration system, that is, repetitions of one-electron transfer to oxygen followed by uptake of one proton.[2] In addition to the four protons consumed to yield two water molecules, another four protons are transported across the mitochondrial inner membrane to generate the electrochemical potential to be used for the synthesis of ATP from ADP.[3,4] The stepwise reduction of an isolated O_2 molecule may imply generation of intermediately reduced oxygen species like $\cdot O_2^-$ $\cdot OOH$, O_2^{--}, $\cdot OOH^-$, $HOOH$, $\cdot O^-$, and $\cdot OH$, which are called active oxygen and very toxic to organisms, but actually no such dangerous intermediates are normally released in the respiration process. Then, how is an O_2 molecule reduced in mitochondria and how is the electron transfer coupled with the proton transport? The purpose of our study is to answer these questions.

The three-dimensional structure of bovine cytochrome *c* oxidase (C*c*O) with $M_r = 2 \times 10^5$ and 13 subunits has been revealed recently with X-ray crystallography.[5] The reaction mechanism of this enzyme has been investigated with various spectroscopic techniques including time-resolved[6–8] and cryo-trapped absorption[9] and EPR[10,11] spectroscopy, but more recently a breakthrough was made with time-resolved resonance Raman (TR^3) spectroscopy by Babcock's group.[12,13] Rousseau's group,[14,15] and our

[1] Institute for Molecular Science, Okazaki National Research Institutes, Myodaiji, Okazaki 444-8585, Japan.

0145-479X/98/0200-0071$15.00/0

group.[16–19] The Cu–S stretching Raman band of the Cu_A center of CcO was also observed in resonance with the 830 nm band.[20] A comprehensive review on the course of progress was given separately[21] and here, some essential conclusions from our TR^3 experiments[19] are explained.

REACTION OF REDUCED *Cc*O WITH O_2

Time-Resolved Resonance Raman Spectra

Resonance Raman (RR) spectroscopy is a technique to observe the vibrational spectra of individual chromophores selectively by tuning the excitation wavelength into an absorption band of molecules. Application of this technique to heme proteins has provided unique and important information on dynamical as well as static structures.[22] In the time-resolved measurements of C*c*O, the reaction was initiated by photolysis of CO-inhibited C*c*O in the presence of O_2, and after a certain delay time (Δt_d) RR spectra were determined. In this TR^3 experiments, a few original tools including a device for simultaneous measurements of Raman and absorption spectra[23] and a sample circulation system for regenerating the reacted enzyme in single recurrence[18] were devised. Since the Raman intensities of the oxygen-associated vibrations are extremely weak, we measured the RR spectra of intermediates for $^{16}O_2$ and $^{18}O_2$ (or $^{16}O^{18}O$) alternately under identical conditions and calculated their difference spectra.

Panel (a) in Fig. 1 shows the TR^3 spectra observed for a H_2O solution at 3°C with Δt_d = 0.1 (A), 0.27 (B), 0.54 (C), 2.7 (D), and 5.4 ms (E), while panel (b) displays similar difference RR spectra observed for a D_2O solution at 3°C with Δt_d = 0.1 (A), 0.54 (B), 2.7 (C), 6.5 (D), and 11 ms (E).[19] The visible absorption spectrum observed simultaneously with spectra (A) is close to that of Compound A obtained with cryogenic techniques.[9] Spectra (a-A) and (b-A) show the Fe–O_2 stretching (ν_{Fe-O_2}) RR bands at 571/544 cm^{-1} for the $^{16}O_2/^{18}O_2$ derivatives. The frequencies and the amount of isotope shift are very close to those seen for HbO_2 and MbO_2.[24] In subsequent stages, new Raman bands appear at 804/764, 785/750, and 356/342 cm^{-1} in (a) but these features are different in (b), as will be discussed later. The 450/425 cm^{-1} pair in spectrum (a-D) corresponds to the 443/417 cm^{-1} pair in spectrum (b-D), and the deuteration shifts suggest that they arise from the Fe–OH(D) stretch ($\nu_{Fe-OH(D)}$) of the Fe^{III}_{a3}–hydroxy heme.[13,15,17] These bands disappear in due course owing to exchanges of the bound $^{18}OH(D)^-$ anion with bulk water. This ν_{Fe-OH} frequency is significantly lower than those of aquametHb and aquametMb at 495 and 490 cm^{-1}, respectively,[25] presumably due to strong interactions between the bound OH^- group and Cu_B.

Spectrum (a-D), which exibits only the 785/750 cm^{-1} pair near 800 cm^{-1}, strongly suggests that the 804/764 cm^{-1} pair precedes the 785/750 cm^{-1} pair. The most unexpected feature in panel (b) is that a single differential band was observed around 800 cm^{-1} (at 804/764 cm^{-1}) at the delay times of Δt_d=0.54 (B) and 2.7 ms (C), contrary to the case for the H_2O solution. The experiments with Δt_d=0.3~0.5 ms for D_2O solutions (data not shown) yielded the 804/764 and 356/342 cm^{-1} bands in a manner similar to spectrum (b-B). This observation once led us to misunderstand[18] that the 785/750 cm^{-1} bands in H_2O were shifted to 796/766 cm^{-1} in D_2O, giving rise to an overlapping band centered around 800 cm^{-1}. However, spectra (b-D) and (b-E) demonstrated that the 785/750 cm^{-1} bands did appear at the same frequencies in D_2O but much later than those in the H_2O solution. It became evident from spectrum (b-D) that the lifetime of the 804/764 cm^{-1} species is so different between the H_2O and D_2O solutions that the 785/750 cm^{-1} species was not generated in D_2O yet at Δt_d=2.7 ms. It is noted that the 356/342 cm^{-1} bands are clearly seen in spectra (B) and (C) at an identical frequency in the H_2O and D_2O solutions.

When the mixed valence CO-bound enzyme, which had only two electrons in a molecule, was used as a starting compound instead of the fully reduced CO-bound enzyme, which had four electrons, the primary intermediate gave the O_2 isotope-sensitive bands at 571/544 cm^{-1}.[26,27] The subsequent intermediate, which is characterized by the difference absorption peak at 607 nm (intermediates fully oxidized), was found to give RR bands at 804/764 and 356/342 cm^{-1} for $^{16}O_2/^{18}O_2$.[19] These bands lasted as long as Δt_d=4.2 ms in H_2O, but the bands at 785/750 and 450/425 cm^{-1} did not appear in this case. These results have proved that the species giving rise to the 804/764 cm^{-1} pair has an oxidation state of heme a_3 higher than that of the 785/750 cm^{-1} species. Hirota et al.[28] carried out similar TR^3 experiments for the reaction intermediates of fully reduced *E. coli* cytochrome *bo* with O_2, and found the O_2 isotope-sensitive bands at 568/535, 788/751, and 361/347 cm^{-1} but failed to find those

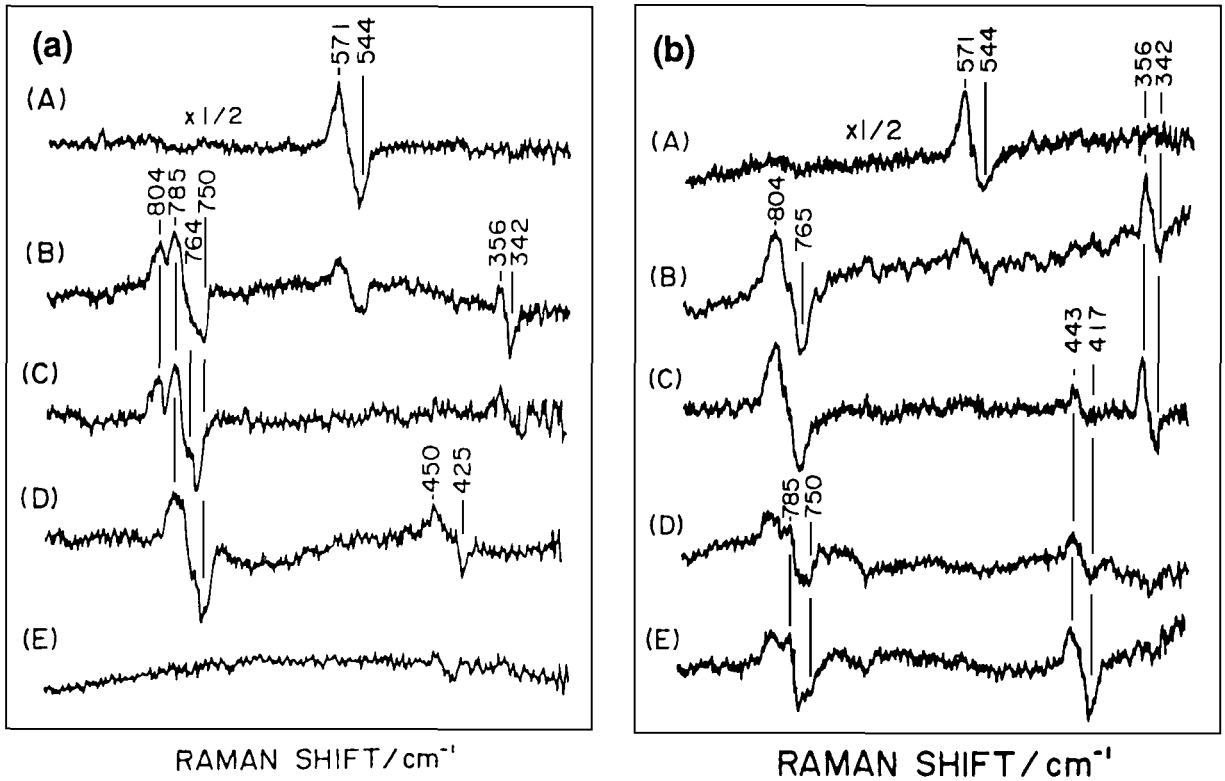

Fig. 1. TR[3] difference spectra of reaction intermediates of C*c*O in H_2O (a) and in D_2O (b). The Raman difference spectra obtained by subtracting the spectrum of the corresponding $^{18}O_2$ derivative from the spectrum of $^{16}O_2$ derivative at each delay time are depicted. Therefore, positive and negative peaks denote the contributions of $^{16}O_2$ and $^{18}O_2$ derivatives, respectively. Delay time after initiation of the reaction is 0.1 (A), 0.27 (B), 0.54 (C), 2.7 (D), and 5.4 ms (E) for (a) and 0.1 (A), 0.54 (B), 2.7 (C), 6.5 (D) and 11 ms (E) for (b). Excitation wavelength, 423 nm; Temperature, 3°C. (Taken from Ref. 19.)

corresponding to the bands of cytochrome aa_3 at 804/764 cm^{-1}.

Binding Geometry of O_2

To determine whether the O_2 of C*c*O adopts the side-on or end-on geometry, Ogura *et al.*[18] examined the RR spectra of $^{16}O^{18}O$-bound C*c*O. The results are shown in Fig. 2, where the observed and simulated isotope-difference spectra are depicted on the left and right sides, respectively, and the combination of the isotope species in the difference calculations is defined in the middle. If $^{16}O^{18}O$ binds to Fe^{II}_{a3} in an end-on geometry, the ν_{Fe-O_2} frequencies for $Fe-^{16}O-^{18}O$ and $Fe-^{18}O-^{16}O$ should be different. Since these two species will be generated by equal amounts, two ν_{Fe-O_2} RR bands should appear. On the other hand, if the binding is of a side-on type, the ν_{Fe-O_2} frequencies for $Fe(^{16}O^{18}O)$ and $Fe(^{18}O^{16}O)$ are identical and are located in the middle of the ν_{Fe-O_2} frequencies of the $^{16}O_2$ and $^{18}O_2$ adducts.

The difference-peak intensities in spectra (B) and (C) are weaker than those in spectrum (A) and peak frequencies are slightly different. If it is assumed, as illustrated in by trace (E), that the $^{16}O_2$ and $^{18}O_2$ species give a single ν_{Fe-O_2} RR band at 571 and 544 cm^{-1}, respectively, but the $^{16}O^{18}O$ species gives two ν_{Fe-O_2} bands at 567 and 548 cm^{-1} with Gaussian band shapes ($\Delta\nu_{1/2}$ = 12.9 cm^{-1}) with relative intensities of 6:6:5:5 for $Fe-^{16}O_2$:$Fe-^{16}O^{18}O$:$Fe-^{18}O^{16}O$:$Fe-^{18}O_2$, the difference calculations for the combinations specified for (A) through (D) yielded the patterns as delineated on the right side. The residuals in subtraction of the simulated spectrum from the observed spectrum are depicted below each simulated spectrum. The calculated difference spectrum for $^{16}O^{18}O - (^{16}O_2+^{18}O_2)/2$ (spectrum D) gives positive peaks at 563 and 552 cm^{-1} and troughs at 574 and 541 cm^{-1}, which are in good

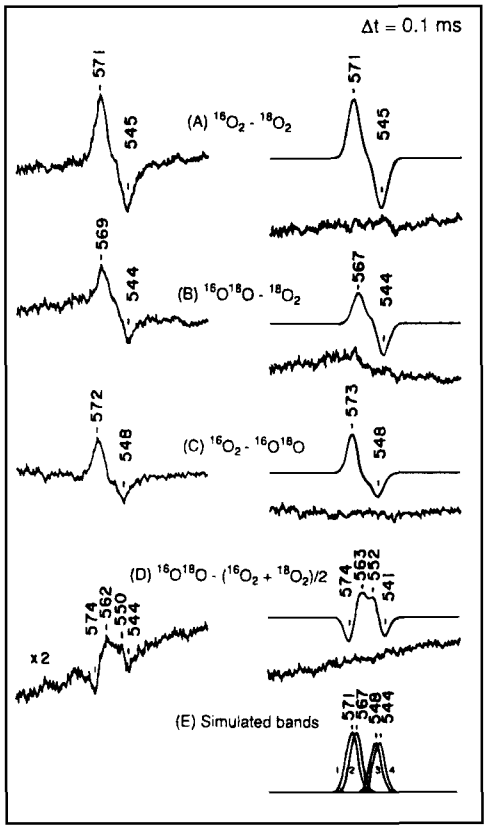

Fig. 2. TR^3 difference spectra in the Fe^{III}-O_2^- stretching region of *Cc*O at the delay time of 0.1 ms. Left side: observed spectra; Right side: calculated spectra; (A) $^{16}O_2$ – $^{18}O_2$; (B) $^{16}O^{18}O$ – $^{18}O_2$, (C) $^{16}O_2$ – $^{16}O^{18}O$; (D) $^{16}O^{18}O$ – ($^{16}O_2$ + $^{18}O_2$)/2. (E) The Fe–$^{16}O_2$ (1), Fe–$^{16}O^{18}O$ (2), Fe–$^{18}O^{16}O$ (3), and Fe–$^{18}O_2$ (4) stretching Raman bands assumed for the simulation. Their peak intensity ratios are 6:6:5:5, and all have a Gaussian band shape with a FWHM of 12.9 cm^{-1}. In the calculation for the $^{16}O^{18}O$ spectrum, (spectrum 2 + spectrum 3)/2 was used. The differences between the observed and calculated spectra are depicted with the same ordinate scale as that of the observed spectra under the individual calculated spectra. Experimental conditions: probe beam, 423 nm, 4 mW; pump beam, 590 nm, 210 mW; accumulation time, 4800 s. (Taken from Ref. 18.)

agreement with the observed spectrum. This suggests that the Fe–O_2 stretching frequencies for the Fe–^{16}O–^{18}O and Fe–^{18}O–^{16}O species are 567 and 548 cm^{-1}, respectively. The magnitude of the isotopic frequency shifts combined with simple normal coordinate calculations allowed us to estimate the Fe–O–O bond angle to be nearly 120° similarly to that in HbO_2 and MbO_2. Thus, this experiment has established that the binding of O_2 to Fe_{a3} in *Cc*O·O_2 is of an end-on type.

Assignments of Transient RR Bands around 800 cm^{-1}

Spectra (B) and (C) in Fig. 1(a) at Δt_d=0.27 and 0.54 ms give two oxygen isotope-sensitive bands around 800 cm^{-1}, and the higher-frequency component arises from the species with the Fe^v oxidation level (compound I of peroxidases). In this frequency region, two kinds of oxygen-associated bands are expected; one is the peroxy O^-– O^- stretch (ν_{OO}) and the other is an ironoxo Fe=O stretch ($\nu_{Fe=O}$). These two modes cannot be distinguished by the $^{16}O_2$ and $^{18}O_2$ isotopic frequency shifts. However, if $^{16}O^{18}O$ is used to produce such intermediates, the distinction would be possible. The peroxy intermediate with $^{16}O^{18}O$ is expected to give an additional ν_{OO} band in the middle of those of the $^{16}O_2$ and $^{18}O_2$ derivatives. In contrast, the oxo intermediate for $^{16}O^{18}O$ is expected to yield two bands at the same frequencies as those seen for the $^{16}O_2$ and $^{18}O_2$ derivatives but with half intensity.

Such a distinction was satisfactorily carried out with $^{16}O^{18}O$ on the 804/764 and 785/750 cm^{-1} bands. The results are shown in Fig. 3(a), where the TR^3 difference spectra observed with Δt_d = 1.1 ms at 5°C for the H_2O and D_2O solutions are presented on the left and right sides, respectively. The various isotope combinations for the difference calculations are defined in the center of the figure. In trace (A) for the H_2O solution, there are two bands at 804 and 785 cm^{-1} for $^{16}O_2$ and they are downshifted to 764 and 751 cm^{-1} with $^{18}O_2$, in agreement with Fig. 1(a-B), obtained in independent experiments with different batches of the enzyme preparations. It is evident that the peak positions and spectral patterns of the difference spectra (B) and (C) in Fig. 3(a) for the H_2O solution are alike and similar to those of spectrum (A) but their intensities are approximately half of those in spectrum (A). The same features are also seen for the D_2O solution (right side). The point to be emphasized is that there is no difference peak in the bottom traces for either the H_2O or D_2O solution. This feature definitely differs from that seen in Fig. 2(D).

These results indicate that only one atom of O_2 is primarily responsible for the two RR bands. Neither the bands at 804/764 nor 785/750 cm^{-1} are assignable to the O–O stretching mode. Although the two sets of RR bands arise from an Fe=O stretch, electronic properties of their hemes seem to be distinct, because only the 804/764 cm^{-1} bands were clearly identified upon Raman excitation at 441.6 nm for Δt_d=0.27 and 1.1 ms, but the 785/750 cm^{-1} bands were not (data

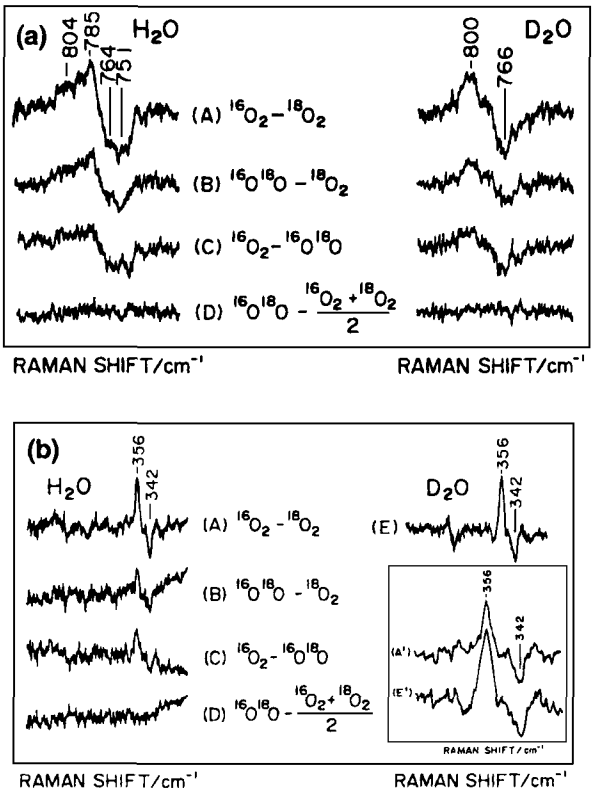

Fig. 3. Higher-resolution TR^3 difference spectra of *Cc*O reaction intermediates in the ~800 cm^{-1} region for the delay time of 1.1 ms (a) and in the ~350 cm^{-1} region for Δt_d = 0.5 ms (b) at 5°C for H_2O (left) and D_2O solutions (right). The ordinate scales are common to all spectra. The spectra combined in the difference calculations are specified in the middle of the figure. Resolution, 0.43 cm^{-1}/channel. The inset in (b) depicts the plots of spectra A and E against the wavenumber axis expanded by 2.5 times.

not shown). Therefore, the simple presence or absence of a hydrogen bond at the $Fe^{IV}=O$ oxygen atom cannot be the origin of the frequency difference between the two oxoiron hemes.

Assignment of the Transient Band around 350 cm^{-1}

Relative intensities of the 804/764 and 356/342 cm^{-1} bands are altered with the delay time. Upon excitation at 441.6 nm, the 356/342 cm^{-1} bands are not enhanced while the 804/764 cm^{-1} bands are clearly observed. Therefore, the two sets of bands are considered to arise from separate molecular species. To clarify the assignment of this band, Ogura *et al.*[18] examined the $^{16}O^{18}O$ effect on the 356/342 cm^{-1} bands. The results are shown in Fig. 3(b), where spectra (A–D) were obtained for the indicated combinations of O_2 isotopes in H_2O solutions and spectrum (E) was obtained for combination (A) in a D_2O solution. Spectra in Figs. 3(a) and 3(b) are represented on the same wavenumber scale. It is noticed that the 356 cm^{-1} band is very narrow. The inset of Fig. 3(b) (spectra A′ and E′) shows redrawing of spectra (A) and (E) against the wavenumber axis expanded by 2.5 times. The 356 cm^{-1} band appears to be somewhat broader in D_2O than in H_2O, but both spectra exhibit a flat region between the positive and negative peaks. This means that the separation between the $^{16}O_2$ and $^{18}O_2$ peaks is larger than their bandwidths, and thus the narrowness of the band is not the consequence of the proximity of the $^{16}O_2$ and $^{18}O_2$ bands. This also means that the peak positions of the difference spectrum correctly represent those of each spectrum.

It is evident from spectrum (b-E) that there are no deuteration effects on the absolute frequencies of the 356/342 cm^{-1} bands. Therefore, this band is neither a Fe–*OOH* nor a Cu–*OH* stretching mode. As was seen for the bands around 800 cm^{-1}, spectra (B) and (C) in Fig. 3(b) do not differ from each other in the shape or position of peaks, which are also close to those of spectrum (A). If the 356/342 cm^{-1} bands arose from the Fe–OOH stretch as proposed by Varotsis *et al.*[13] the frequency difference between the Fe–$^{16}O^{18}OH$ and Fe–$^{16}O^{16}OH$ stretches and that between the Fe–$^{18}O^{16}OH$ and Fe–$^{18}O^{18}OH$ stretches should be as large as 2.5 cm^{-1} unless the Fe–O–O bond angle is close to 90°, and there should be some difference peaks in Fig. 3(b-D) as seen for the $Fe–O_2$ adduct in Fig. 2(D). Actually, however, there is no difference peak in spectrum (D) in Fig. 3(b). Therefore, only one oxygen atom from the O_2 molecule is primarily responsible for the 356 cm^{-1} band, too.

For an oxoiron heme, there should be three oxygen isotope-sensitive vibrations; one is the Fe=O stretch and the other two should contain movements of the oxygen atom perpendicular to the Fe=O bond. Since the Fe=O stretching Raman band is present separately, the 356 cm^{-1} band is assigned to the His-Fe=O bending vibration. When the Fe=O bond is perpendicular to the heme plane, the Fe=O stretch belongs to the A_1 species of C_{4v} and is Raman active, but the His–Fe=O bending belongs to the E species of C_{4v} and is Raman inactive. In fact, for compound II of horseradish peroxidase, the His–Fe=O bending mode has not been detected with any excitation wavelength of 441.6, 427.0, 413.1, and 406.7 nm. If the

N–Fe and Fe=O bonds are distorted from a straight line, the His–Fe=O bending would become Raman active. It is highly likely that the 356 cm^{-1} band of CcO arises from a distorted oxoiron heme, in which the proximal histidine is distorted, and its Fe=O stretch appears around 800 cm^{-1}. The appearance of the bending band seems to be characteristic of cytochrome oxidases having proton pumping activity. If this is the case, the distortion energy of heme might be used to translocate the vector protons in the protein.

REACTION OF OXIDIZED *Cc*O WITH H_2O_2

The reaction of ferric heme proteins with H_2O_2 usually yields the Fe^V-level intermediate first, which is then successively reduced to the Fe^{IV} and Fe^{III} oxidation levels. The reaction of oxidized CcO with H_2O_2 has been extensively studied with visible absorption,[29] EPR,[30] and RR spectroscopy.[31-33] Studies on the visible absorption spectra suggested that the "607 nm" absorbing form is generated first and is then replaced by the "580 nm" absorbing form. These intermediates are defined by the peak position of intermediates in their difference spectra in reference to that of the resting enzyme. The rate of formation of the 607 nm form was found to be proportional to the concentration of H_2O_2 and was considered to be the primary intermediate in this reation. This means that the 607 nm form has the heme a_3 with the Fe^V oxidation level. When the concentration of H_2O_2 is increased, the 580 nm form is developed rapidly. This is interpreted in the following way. Under high concentrations of H_2O_2, the 607 nm form develops much faster and the extra H_2O_2 acts as a reductant to the 607 nm form to yield the 580 nm form, which has the heme a_3 with the Fe^{IV} oxidation level. Accordingly, the relative populations of the 607 nm and 580 nm forms can be regulated by the concentration of H_2O_2 and pH.[33]

Figure 4 shows the absorption (right) and Soret-excited RR spectra (left) of intermediates which were measured simultaneously with an improved Raman/absorption simultaneous measurement device.[31] In this experiment the concentrations of reaction intermediates in question are retained in a steady state for a certain period of time by adding H_2O_2 with a constant rate to the circulating solution. The upper spectra were obtained under the conditions where the 607 nm form is dominant, while the lower spectra were obtained under the conditions where the 580 nm form is dominant. Both RR spectra are represented as the difference

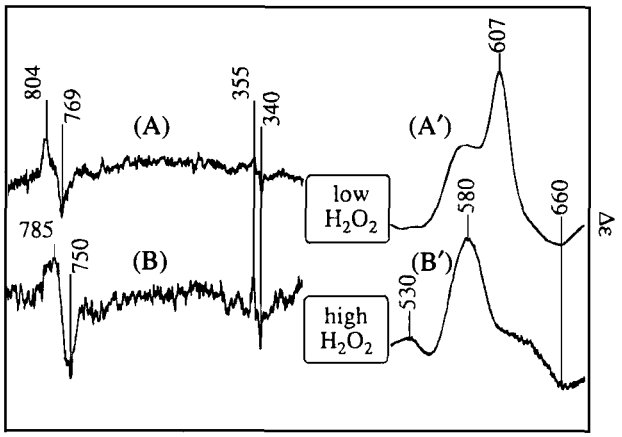

Fig. 4. The steady-state Raman/absorption simultaneously observed spectra of the "607 nm" and "580 nm" forms of cytochrome *c* oxidase at pH 8.5. Raman spectra A and B are shown as a difference of $H_2{}^{16}O_2$ compound minus $H_2{}^{18}O_2$ compound. Spectra A/A': laser, 427 nm, 2.5 mW; accumulation time, 3 × 2400 sec for each isotope; cytochrome *c* oxidase, 50 μM; initial concentration of H_2O_2, 1 mM, Spectra B/B': laser power, 7.5 mW; accumulation time, 3 × 800 sec for each isotope; cytcohrome *c* oxidase, 10 μM; initial concentration of H_2O_2, 5 mM. Absorption spectra are represented as a difference with regard to the spectrum of the resting enzyme; ordinate full scale $\Delta\varepsilon$ = 11.7 mM^{-1} cm^{-1}; path length 0.6 mm. (Taken from Ref. 31.)

between the derivatives obtained from $H_2{}^{16}O_2$ and $H_2{}^{18}O_2$, and accordingly positive and negative peaks correspond to the vibrations associated with ^{16}O and ^{18}O, respectively. It is noted that when the 607 nm form is dominant, the 804/769 cm^{-1} bands are clearly observed and when the 580 nm form is dominant, broad bands centered around 785/750 cm^{-1} and sharp bands at 355/340 cm^{-1} are intensified. The intensity of the 355/340 cm^{-1} bands relative to those of the 804/769 and 785/750 cm^{-1} bands were varied with each experiment. This strongly suggested that the species giving rise to the 355/340 cm^{-1} bands also gives a difference band around 800/760 cm^{-1} but is different from the two species giving rise to the 804/769 and 785/750 cm^{-1} bands. The 355/340 cm^{-1} species seems to have an absorption spectrum similar to that of the 580 nm form. This implies that the 580 nm form consists of multiple intermediate species.[33] It is stressed that all these oxygen isotope-sensitive bands are identical with those observed in the reduction of O_2.

Hitherto the 607 nm form has been believed to be a peroxo species, namely, Fe–O–O–X (X = H or Cu_B). Since both the O^-–O^- and Fe=O stretching frequencies are located around 800 cm^{-1}, it is impossible to determine which type of vibrations was observed

for the 607 nm form in Fig. 4. To sort out the two possible modes, experiments using $H_2{}^{16}O{}^{18}O$ have been performed. The results are shown in Fig. 5, where RR spectra of the 607 nm form excited at 607 nm are displayed for intermediates derived with $H_2{}^{16}O_2$ (A), $H_2{}^{18}O_2$ (B), and $H_2{}^{16}O{}^{18}O$ (C).[32] The band of the $H_2{}^{16}O_2$ derivative at 803 cm^{-1} (A) is shifted to 769 cm^{-1} for the $H_2{}^{18}O_2$ derivative (B), while other bands arising from the porphyrin macrocycle remain unshifted. This is most clearly seen in the difference spectrum (D) [= spectrum (A) − spectrum (B)]. The inset shows the same difference spectrum in an extended spectral range (930–550 cm^{-1}). It is evident that there is no other oxygen-associated band in the frequency region involving the 785/750 cm^{-1} bands. Consequently, this exclusively indicates that the 607 nm absorbing form gives rise to the 803/769 cm^{-1} Raman bands.

In spectrum (C) for the $H_2{}^{16}O{}^{18}O$ derivative, there are two bands at 803 and 769 cm^{-1}, and their intensities relative to the porphyrin bands are reduced to half of those in spectra (A) and (B). This is most clearly seen by the difference spectrum (E) [= spectrum (C) − (spectrum (A) + spectrum (B))/2], which exhibits no band in the 700–900 cm^{-1} region. This means that the 803/769 cm^{-1} bands arise from a species which has a single oxygen atom on the heme iron. Consequently, the peroxide structure (Fe–O–O–X), postulated for the 607 nm form, was proved to be no longer valid.

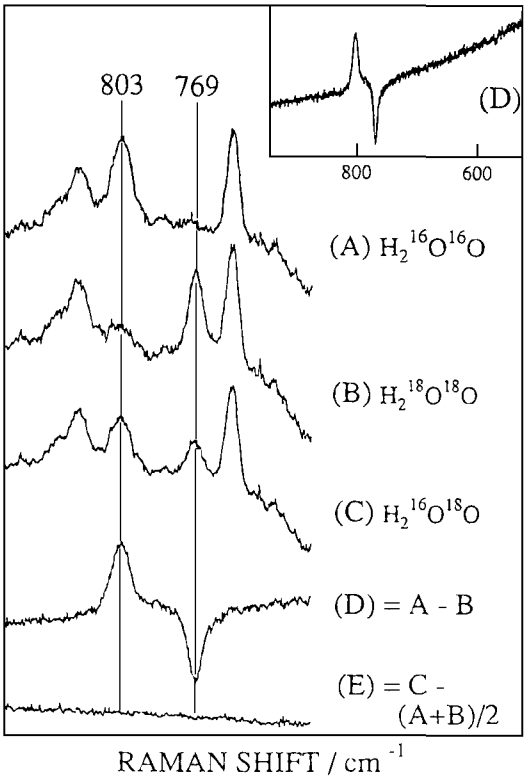

Fig. 5. The 607-nm excited steady-state RR spectra in the 800 cm^{-1} region of the "607 nm" form of C*c*O formed in the reaction of the oxidized enzyme with hydrogen peroxide. Hydrogen peroxide used are $H_2{}^{16}O_2$ (A), $H_2{}^{18}O_2$ (B), and $H_2{}^{16}O{}^{18}O$ (C). Spectra D and E show difference spectra: spectrum D = spectrum A − spectrum B; spectrum E = spectrum C − (spectrum A + spectrum B)/2. The inset (spectrum D) is the same as spectrum D in the main frame but shows the full frequency range measured. Experimental conditions; cross section of flow cell, 0.6 × 0.6 mm^2; slit width, 4.2 cm^{-1}; laser 607 nm, 100 mW at the sample; total accumulation time, 78, 78, and 156 min for spectra A, B, and C, respectively, and 160 min for the resting enzyme; cytochrome *c* oxidase, 50 μM, pH 7.45. (Taken from Ref. 32.)

SUMMARY OF REACTION MECHANISM

The reaction intermediates of C*c*O characterized by RR spectroscopy and other spectroscopic techniques are inter-related in Fig. 6, where the oxygen-associated frequencies for $^{16}O/^{18}O$ in two kinds of

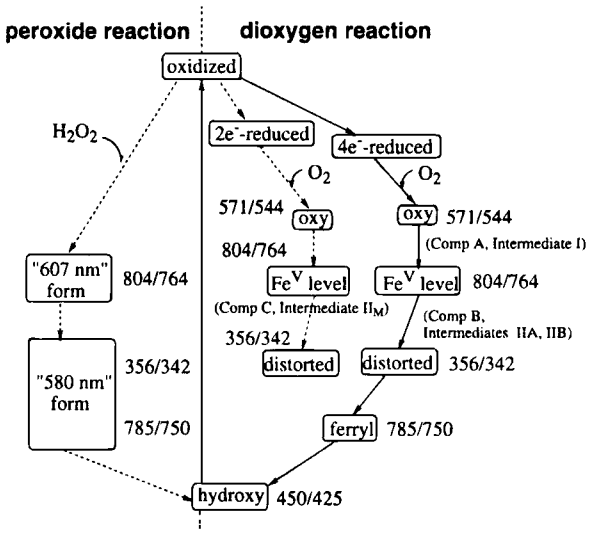

Fig. 6. Reaction mechanism of cytochrome *c* oxidase, inter-relations of intermediates obtained with different techniques, and the specific oxygen-associated vibrational frequencies ($^{16}O_2$ derivatives/$^{18}O_2$ derivatives in cm^{-1} unit) of individual intermediates. In the dioxygen reaction the fully reduced (4e⁻-reduced) and the mixed-valence (2e⁻-reduced) species are contained. The peroxide reacion gives rise to two absorption forms, but the "580 nm" form is of multiple species and is further sorted out by vibrational frequencies. The "peroxy" and "ferryl" forms in the reverse reaction are presumably the same as the "607 nm" and 580 nm "forms of the peroxide reaction, respectively.

reactions, that is, dioxygen cycle (right) and peroxide cycle (left), are also specified. The primary intermediate in the reaction of reduced C*c*O with O_2, which has been called Compound A, has now been demonstrated to be an O_2 adduct of heme a_3 with ν_{Fe-O_2} at 571 cm^{-1}. The binding of O_2 is of the end-on type with an Fe–O–O bond angle of ca 120°. Compound B is a mixture of the subsequent intermediates with oxygen isotope-sensitive bands at 804, 356, and 785 cm^{-1} for $^{16}O_2$ in the order of their appearance. The intermediates which are generated in the reaction of mixed-valence enzyme with O_2 give the oxygen isotope-sensitive bands at 804 and 356 cm^{-1} in addition to the 571 cm^{-1} band. Therefore, it is established that the 804 cm^{-1} species has a higher oxidation state than the 785 cm^{-1} species which is no doubt assigned to the $Fe^{IV}=O$ heme a_3 species. The final intermediate in the dioxygen cycle has an Fe^{III}_{a3}–OH^- heme with ν_{Fe-OH} RR band at 450 cm^{-1}. This OH^- group is exchangeable with bulk water. This species would correspond to the so-called pulsed form.

In the reaction of oxidized enzyme with H_2O_2, the first intermediate, the 607 nm form, has long been thought to have the peroxo Fe_{a3}–O–O–X structure, but RR experiments demonstrated that the O–O bond has already been cleaved. The subsequent intermediates give a broad difference peak at 580 nm and seem to have multiple components. RR spectroscopy can sort out two species within the 580 nm form. One gives the oxygen isotope-sensitive bands at 356 and ~800 cm^{-1} and the other gives the band at 785 cm^{-1}. The latter is unquestionably assigned to the $Fe^{IV}=O$ stretching mode. The 356 cm^{-1} band is assigned to the His-Fe=O bending mode of a distorted oxoiron heme whose Fe=O stretching band is overlapped around 800 cm^{-1}.

Figure 7 illustrates possible structures of the heme a_3–Cu_B binuclear center of reaction intermediates categorized by the oxidation level. The $1e^-$(Fe^{III}–O_2^-, Cu_B^I) and the $4e^-$ (Fe^{III}–OH^-, Cu_B^{II}) reduced intermediates have been established. There is no doubt about the formation of normal $Fe^{IV}=O$ heme in the $3e^-$ reduced state. This species gives rise to the 785/750 cm^{-1} Raman bands and the difference absorption peak around 580 nm. Some controversy is currently present in the $2e^-$ reduced state. Since the O–O bridging structure is incompatible to the Raman results, there would remain five possible structures; (1) an $Fe^{IV}=O$ heme with an amino acid radical ($X^{\cdot+}$) like compound ES of cytochrome *c* peroxidase, and (2) an $Fe^{IV}=O$ porphyrin π cation radical like compound I of horseradish peroxidase, (3) an $Fe^{v}=O$ heme with d^3 iron, (4) an $Fe^{IV}=O$ heme with $Cu_B^{III}=O$, and (5) an $Fe^{IV}=O$ heme with a Cu_B^{II}–$O^{\cdot}$ (oxygen radical). Reaction pathways (2) and (3) involve the heterolysis of the O–O bond, while pathways (4) and (5) involve its homolysis. Only pathway (1) can proceed through either heterolytic or homolytic cleavage of the O–O bond.

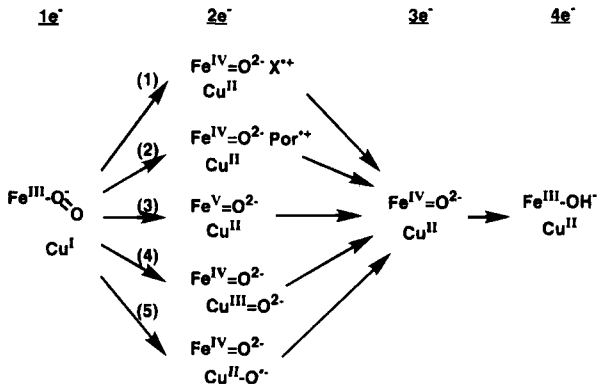

Fig. 7. Possible pathways for reduction of O_2 bound to the heme a_3–Cu_B binuclear center of cytochrome *c* oxidase. $1e^-$, $2e^-$, $3e^-$, and $4e^-$ mean the one-, two-, three-, and four-electron reduced species, respectively. "Por," "Por$^{\cdot+}$," and $X^{\cdot+}$ mean nonradical porphyrin, its π cation radical, and an amino acid cation radical, respectively.

For intermediates in the reaction of reduced C*c*O with O_2, there have been no EPR data which exhibit the $g=2$ signal arising from an amino acid radical. Therefore, there is no positive support for pathway (1). Porphyrin π cation radicals usually have singificantly reduced Soret absorbance compared with that of nonradical porphyrins and exhibit some characteristic RR bands for porphyrin vibrational modes. Since the Soret absorption of the 804/764 cm^{-1} species is of ordinary intensity and its RR spectrum in the higher frequency region is similar to those of nonradical porphyrins, the possibility that this species contains a porphyrin π cation radical may be ruled out. When homolyric cleavage of the O–O bond takes place immediately after instantaneous formation of the Fe^{III}–O^-–O^-–Cu_B^{II} structure, two oxometal centers, that is, $Fe^{IV}=O$ and $Cu_B^{III}=O$ will be generated as shown in pathway (4). The $Cu_B^{III}=O$ could be a Cu_B^{II}–$O^{\cdot}$ oxygen radical as assumed in pathway (5). It is noted that, for pathways (1), (4), and (5), the hemes of the $2e^-$ and $3e^-$ reduced species would have basically common electronic properties and cannot explain the selective enhancement of the 804/764 cm^{-1} band at 441.6 nm excitation in coexistence of the 804/764 and 785/750 cm^{-1} species, unless the amino acid radical or the

Cu_BO unit interacts so strongly with the Fe=O heme in the $2e^-$ reduced state to raise its stretching frequency by 20 cm^{-1}, to change the heme electronic state, and to make the EPR signal extremely weak via antiferromagnetic coupling.

On the other hand, when one tries to oxidize an Fe^{IV}=O heme by one unit, it cannot be predicted *a priori* whether an electron is removed from the metal ion or from the macrocycle. For an Fe^{IV} = O heme there are two electrons in the d_{xz} and d_{yz} orbitals of the iron atom. It is not known whether they are energetically higher or lower than the HOMO of the porphyrin macrocycle with a_{1u} or a_{2u} symmetry. When some electron-withdrawing substituents are attached to the heme, the a_{1u} or a_{2u} orbital is energetically lowered[34] and may become lower than the iron d_{xz} and d_{yz} orbitals. In this case an electron would be taken out of the iron orbital, generating the Fe^V state. The formyl substituent of heme A is strongly electron-withdrawing. Consequently, the formation of the Fe^V heme remains as a likely candidate for the $2e^-$ reduced intermediate of aa_3-type cytochromec *c* oxidases, and this is compatible with the fact that the 804 cm^{-1} band is not observed for cytochrome *bo* which lacks the formyl substituent.[28]

ACKNOWLEDGMENT

This study was supported by Grant-in-Aids for Scientific Research on Priority Areas (Molecular Biometallics, 08249106) from the Ministry of Education, Science, Sports and Culture, Japan.

REFERENCES

1. M. Wikstrom, K. Krab, and M. Saraste, *Cytochrome Oxidase; A Synthesis,* Academic Press, New York (1981).
2. G. T. Babcock and M. Wikstrom, *Nature* **356**, 301–309 (1992).
3. M. Wikstrom, *Proc.Natl. Acad. Sci. USA* **78**, 4051–4055 (1981).
4. N. Sone and P. C. Hinkle, *J. Biol. Chem.* **257**, 12600–12604 (1982).
5. T. Tsukihara, H. Aoyama, E. Yamashita, T. Tomizaki, H. Yamaguchi, K. Shinzawa-Itoh, R. Nakashima, R. Yaono and S. Yoshikawa, *Science* **269**, 1069–1074 (1995).
6. Y. Orii, *Ann. N.Y. Acad. Sci.* **550**, 105–117 (1988).
7. R. S. Blackmore, C. Greenwood, and Q. H. Gibson, *J. Biol. Chem.* **266**, 19245–19249 (1991).
8. M. Oliveberg and B. G. Malmstrom, *Biochemistry* **31**, 3560 (1992).
9. B. Chance, C. Saronio, and J. S. Leigh, Jr., *J. Biol. Chem.* **250**, 9226–9237 (1975).
10. G. M. Clore L.-E. Andreasson, B. Karlsson, R. Aasa, and B. G. Malmstrom, *Biochem. J.* **185**, 139–154 (1980).
11. D. F. Blair, S. N. Witt, and S. I. Chan, *J. Am. Chem. Soc.* **107**, 7389–7399 (1985).
12. C. Varotsis, W. H. Woodruff, and G. T. Babcock *J. Am. Chem. Soc.* **111**, 6439 (1989) **112**, 1297 (1990).
13. C. Varotsis, Y. Zhang, E. H. Appelman, and G. T. Babcock, *Proc. Natl. Acad. Sci. USA* **90**, 237 (1993).
14. S. Han, Y. -C. Ching, and D. L. Rousseau, *Proc. Natl. Acad. Sci. USA* **87**, 2491–2495 (1990).
15. S. Han, Y. -C. Ching, and D. L. Rousseau, *Nature* **348**, 89–90 (1990).
16. T. Ogura, S. Takahashi, K. Shinzawa-Itoh, S. Yoshikawa, and T. Kitagawa, *J. Am. Chem. Soc.* **112**, 5630–5631 (1990).
17. T. Ogura, S. Takahashi, K. Shinzawa-Itoh, S. Yoshikawa, and T. Kitagawa, *Bull. Chem. Soc. Jpn.* **64**, 2901–2907 (1991).
18. T. Ogura, S. Takahashi, S. Hirota, K. Shinzawa-Itoh, S. Yoshikawa, E. H. Appelman, and T. Kitagawa, *J. Am. Chem. Soc.* **115**, 8527–8536 (1993).
19. T. Ogura, S. Hirota, D. A. Proshlyakov, K. Shinzawa-Itoh, S. Yoshikawa, and T. Kitagawa, *J. Am. Chem. Soc.* **118**, 5443–5449 (1996).
20. S. Takahashi, T. Ogura, K. Shizawa-Itoh, S. Yoshikawa, and T. Kitagawa, *Biochemistry* **32**, 3664–3670 (1993).
21. T. Kitagawa and T. Ogura, *Prog. Inorg. Chem.* **45**, 431–479 (1997).
22. T. Kitagawa and T. Ogura, *Adv. Spectrosc.* **21**, 139–188 (1993).
23. T. Ogura and T. Kitagawa, *Rev. Sci. Instrum.* **59**, 1316–1320 (1988).
24. K. Nagai, T. Kitagawa, and H. Morimoto, *J. Mol. Biol.* **136**, 271–289 (1980).
25. S. A. Asher and T. M. Schuster, *Biochemistry* **18**, 5377–5387 (1979).
26. S. Han, Y. -C. Ching, and D. L. Rousseau, *J. Am. Chem. Soc.* **112**, 9445–9450 (1990).
27. C. Varotsis, W. H. Woodruff, and G. T. Babcock, *J. Biol. Chem.* **265**, 11131–11136 (1990).
28. S. Hirota, T. Mogi, T. Ogura, T. Hirano, Y. Anraku, and T. Kitagawa, *FEBS Lett.* **352**, 67–70 (1994).
29. T. V. Vygodina and A. A. Konstantinov, *Ann. N.Y. Acad. Sci.* **550**, 124–138 (1988).
30. M. Fabian and G. Palmer, *Biochemistry* **34**, 13802–13810 (1995).
31. D. A. Proshlyakov, T. Ogura, K. Shinzawa-Itoh, S. Yoshikawa, and T. Kitagawa, *Biochemistry* **35**, 76–82 (1996).
32. D. A. Proshlyakov, T. Ogura, K. Shinzawa-Itoh, S. Yoshikawa, E. H. Appelman, and T. Kitagawa, *J. Biol. Chem.* **269**, 29385–29388 (1994).
33. D. A. Proshlyakov, T. Ogura, K. Shinzawa-Itoh, S. Yoshikawa, and T. Kitagawa, *Biochemistry* **35**, 8580–8586 (1996).
34. H. Fujii ad K. Ichikawa, *Inorg. Chem.* **31**, 1110–1112 (1992).